

Electron transfer reactions in clusters: The effect of polar solvents on the (2p3s) Rydberg state of azabicyclo-octane

C. F. Dion and E. R. Bernstein

Citation: *The Journal of Chemical Physics* **104**, 2891 (1996); doi: 10.1063/1.471111

View online: <http://dx.doi.org/10.1063/1.471111>

View Table of Contents: <http://aip.scitation.org/toc/jcp/104/8>

Published by the *American Institute of Physics*

COMPLETELY

REDESIGNED!



**PHYSICS
TODAY**

Physics Today Buyer's Guide
Search with a purpose.

Electron transfer reactions in clusters: The effect of polar solvents on the $(2p3s)$ Rydberg state of azabicyclo-octane

C. F. Dion and E. R. Bernstein

Department of Chemistry, Colorado State University, Fort Collins, Colorado 80523

(Received 25 September 1995; accepted 16 November 1995)

$(1+1)$ mass resolved excitation spectra are reported for the $(2p3s) \leftarrow (2p)^2$ Rydberg transition of azabicyclooctane (ABCO) van der Waals clusters. The solvent molecules employed in this study are mostly polar. The polar solvent cluster spectra are red shifted from those of the bare molecule ABCO by more than 500 cm^{-1} in most cases. This large increase in the interaction energy of the ABCO molecule Rydberg state in polar solvent clusters with respect to that of the ground state ABCO cluster is due to an exchange delocalization or electron transfer interaction for the excited state cluster. The ABCO Rydberg state electron is delocalized into the available (virtual) orbitals of the polar solvent molecule. Relaxation dynamics are measured for the generation of the electron transfer state of the cluster. This behavior is similar to that characterized for other cyclic amines in polar solvent clusters. © 1996 American Institute of Physics. [S0021-9606(96)02708-6]

I. INTRODUCTION

Spectroscopic studies of van der Waals clusters have contributed significantly to our understanding of intermolecular interactions and ground and excited electronic state dynamics. This information has provided insight into both molecular and condensed phase systems.¹ Solvation effects for valence transitions comprise the bulk of these data; they demonstrate that the higher polarizability of an excited electronic state with respect to the ground state results in an increased binding energy for the excited state cluster. The different ground and excited state binding energies result in an overall transition energy red shift for the cluster which can be modeled based on simple empirical potential energy forms.^{2,3}

In the last few years our laboratory has made similar studies of the microscopic van der Waals cluster solvation interaction and dynamics for Rydberg electronic states.⁴⁻⁹ As one might anticipate, Rydberg excited states behave very differently from valence excited states with regard to microscopic solvation. For nonpolar solvents the dominant interaction for the diffuse and expanded electronic states turns out to be an exchange repulsion (Pauli exclusion principle) which overwhelms the standard ground state van der Waals (dispersion, dipole-dipole, dipole-induced dipole, etc.) forms to generate an overall blue shift of the cluster transition energy. The electron in the expanded excited state orbital ($2p3s$ configuration) is repelled by the closed shells of nonpolar solvent species (e.g., rare gases, linear and cyclic alkanes). This repulsive interaction is nearly sufficient in some instances to reduce the binding energy of an excited state cluster to zero. Demonstrations of these shifts have appeared for aza- and diazabicyclooctane ($\text{C}_7\text{H}_{12}\text{N}$ -ABCO and $\text{C}_6\text{H}_{12}\text{N}_2$ -DABCO), dioxane, and hexamethylenetetramine ($\text{C}_6\text{H}_{12}\text{N}_4$ -HMT).

The low lying Rydberg state transitions of these molecules are typically characterized as $(2p3s) \leftarrow (2p)^2$ but two electron transitions of the form $(3s)^2 \leftarrow (2p)^2$ can also play an important role in these excited states.⁹ In general these

low lying Rydberg states are long lived ($\sim 1 \mu\text{s}$) and decay to triplet states that are less than 800 cm^{-1} to lower energy.⁹ Cluster formation reduces the symmetry of the chromophore system and allows for intermolecular heavy-atom effects to enhance the spin-orbit interaction, and thereby increases the intersystem crossing rate for the $^1R_1 \rightarrow ^3R_n$ transition. Reduced excited state lifetimes, cluster dissociation, and a required increased ionization energy for the clusters or bare molecules are all consequences of this rather straightforward behavior for Rydberg state van der Waals clusters of saturated amines and ethers.

The situation is dramatically different for these chromophore solvated by polar and unsaturated solvent molecules. In such cases one observes large red shifted cluster transitions ($\sim 500 \text{ cm}^{-1}$), rapid decays ($\sim 100 \text{ ns}$) to long lived states, and increased ionization energies for the long lived states. These phenomena are associated with solvents that have available empty orbitals at or near the Rydberg state energy. Amine, ether, and aromatic solvents fall into this general category. This behavior is readily explained by an electron delocalization or electron transfer between the Rydberg chromophore molecule and the solvent. The long lived lower energy state that appears after $\sim 100 \text{ ns}$ for DABCO is an electron or charge transfer state.⁹

In this report we show that the "solute-solvent" electron transfer in one-to-one clusters is a more general phenomenon than has already been observed for DABCO⁹ and HMT.⁶ Surely such behavior takes place in condensed phases as well and must be responsible for a considerable body of photochemistry. ABCO/solvent clusters are generated in a supersonic expansion and detected and analyzed by one- and two-color mass resolved excitation spectroscopy (MRES). The solvents employed that generate a low lying electron transfer state are either polar or unsaturated. Specifically, these solvents include acetonitrile, 1,4-dioxane, ammonia, dimethyl ether, tetrahydropyran (THP), ABCO, benzene, and ethylene. Argon and cyclohexane are used as comparison solvents representing nonpolar molecules.

The spectra of these clusters are characterized by shifts from bare ABCO features, linewidths, and time dependent intensities. As for the cases of DABCO and HMT, the interactions in and behavior of these clusters can be understood on the basis of a number of limiting empirical potential forms; van der Waals (dispersion), dipole- (induced) dipole, Pauli exclusion/exchange repulsion, attractive electron exchange (delocalization), and energy transfer (off resonance exchange).

II. EXPERIMENTAL PROCEDURES

The study of the affect of solvation on Rydberg states is best carried out in cold gas phase clusters. Supersonic jet expansion and time of flight mass spectroscopy detection have become the main tools for such studies, and their practice in our laboratory in this regard has been previously detailed.¹⁰ We briefly describe the procedure as it pertains to these experiments below.

ABCO is placed in a pulsed nozzle and expanded into a vacuum chamber with ~ 50 psi He. Solvent gas is premixed with the He expansion gas at about 0.5% to 5.0% (by pressure) as is required for acceptable signal levels. The (1+1) MRES are generated by a Nd/YAG pumped dye laser using DCM and LDS dye solutions or a mixture of the two as appropriate to cover the wavelength region scanned. The dye fundamental is doubled and mixed with 1.064 μm Nd/YAG fundamental to achieve the necessary wavelengths.

The ionization thresholds for the ABCO lowest ($2p3s$) Rydberg singlet and triplet states can be determined in similar experiments. The ionization threshold of these states is measured in a two color (1+1)-MRES experiment. The excitation laser is tuned to the Rydberg singlet (1R_1) origin transition and a second laser with C460 dye solution as the active medium is used for ionization. The ionization threshold of the triplet state (3R_n) is determined using a C440 solution in the dye laser. To determine the triplet state ionization energy, a delay of $\sim 0.5 \mu\text{s}$ between the excitation and ionization lasers is required to allow the intersystem crossing process to occur and the singlet Rydberg state population to decay sufficiently so that the triplet state is the only state available to ionize.

The lifetimes of ABCO and its clusters in the 1R_1 , 3R_n , and electron transfer states can be determined using a two color MRES scheme with time delay between the two lasers. Lifetimes are measured with the ionization laser set about 100 cm^{-1} above threshold ionization value for the appropriate Rydberg state.

III. RESULTS

A. Calculated cluster geometries

In order to aid in the interpretation of cluster spectra and to appreciate the microscopic details of clusters behavior, we have performed, as done for other systems in similar studies,^{1,2} empirical potential energy calculations of possible cluster geometries. The potential forms and parameters are the same as those used previously; Lennard-Jones-Coulomb

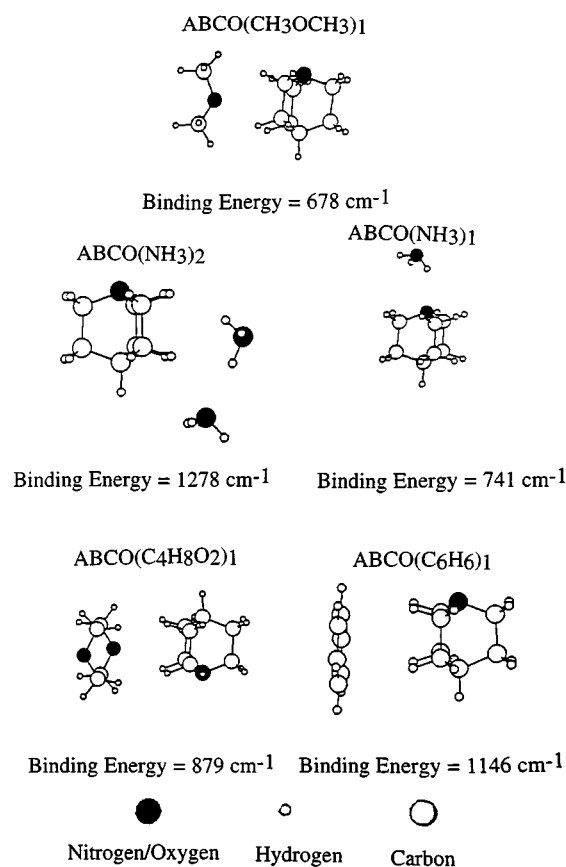


FIG. 1. Most stable conformations of ABCO(CH₃OCH₃)₁, ABCO(NH₃)₂, ABCO(NH₃)₁, ABCO(dioxane)₁, and ABCO(benzene)₁. The binding energy of each cluster is given below the structure. These conformers are calculated with a Lennard-Jones 6-12 plus Coulomb potential using molecular input geometries generated in a MOPAC 6.0 calculation using an AM1 Hamiltonian. Except for the ABCO(NH₃)₁ cluster, the most stable cluster conformation is the one in which the solvent molecule is located on the side closest to the ethylene bridges of the ABCO molecule. The ABCO(NH₃)₁ cluster is similar to the DABCO/polar solvent clusters in which the most stable geometry is the one in which the solvent molecule is located just off the C₃ axis and near the nitrogen end of the molecule.

for atom-atom interaction^{1,3-6,11,12} and MOPAC 6.0 AM1 calculations¹³ for geometries and partial atomic charges. As expected, based on the results for dioxane and DABCO, the ABCO molecule has three basic solvation positions; at the nitrogen and of the molecule (but off the threefold axis); at the "edge" of the molecule between two ethylene bridges; and at the tertiary carbon position (again off the threefold axis).

For small, nonpolar molecules and rare gases, the edge solvation position of DABCO generates the most stable (largest binding energy) cluster.⁵ For polar solvent/DABCO clusters, the nitrogen end solvent position generates the most stable cluster.⁹ The situation is different for ABCO clusters as shown in Fig. 1. In this instance, small solvent molecules (e.g., ammonia) have the most stable interaction with the nitrogen end of ABCO, but larger solvents (e.g., dioxane, benzene, ether, etc.) interact most strongly with the edge position of ABCO. The ABCO (C₆H₆)₁ cluster has two general conformers; the edge and the tertiary carbon solvation sites

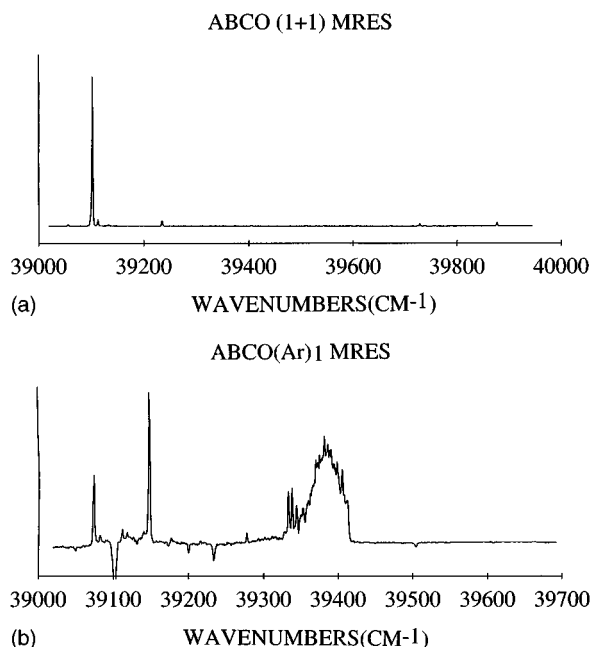


FIG. 2. (a) The (1+1) mass resolved excitation spectrum of ABCO is given in the region of the $\text{ABCO}(2p3s)$ Rydberg state. This spectrum is borrowed from Ref. 4. (b) The (1+1) MRES of $\text{ABCO}(\text{Ar})_1$ in the $\text{ABCO}(2p3s)$ region showing the origin of $\text{ABCO}(\text{Ar})_1$. The blue shift of the origin is due to the repulsive Pauli exclusion interaction between the excited Rydberg electron and the closed shell of the Ar atom. The red shifted feature is due to a cluster with the Ar atom coordinated to the tertiary carbon end of ABCO (see Ref. 4 for a complete explanation of these features).

are occupied as though some “hydrogen bonding” between ABCO and the π -system were occurring. These geometries will surely affect our reasoning for the elucidation of the electron transfer behavior of ABCO/polar solvent clusters.

B. Spectra

1. ABCO bare molecule and $\text{ABCO}(\text{Ar})_1$

The spectrum of ABCO is presented in Fig. 2. The 0_0^0 transition at $39\,101.1\text{ cm}^{-1}$ is the most intense feature within the first 500 cm^{-1} of the spectrum. The spectrum is obtained with two-color resonant ionization and is mass detected.⁵ Figures 2(a) and 2(b) also present the spectrum of the $\text{ABCO}(\text{Ar})_1$ clusters, all three of which can be observed. As

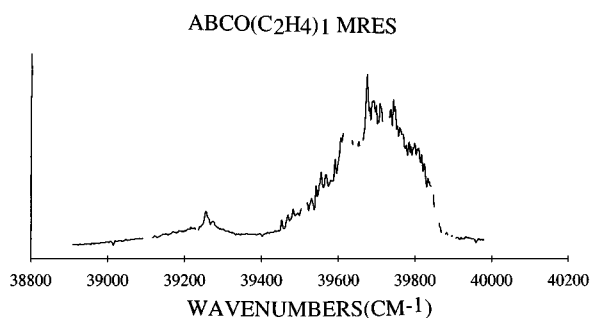


FIG. 3. The (1+1) MRES of $\text{ABCO}(\text{C}_2\text{H}_4)_1$ is presented. The gaps in the trace are caused by strong absorption due to 1,4 dioxane, which is used as a line-up molecule for this region.

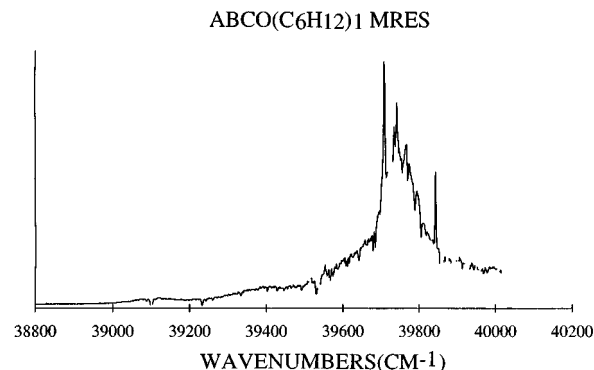


FIG. 4. The (1+1) MRES of $\text{ABCO}(\text{C}_6\text{H}_{12})_1$ ($2p3s$) Rydberg state. The blue shift (approximately 600 cm^{-1}) of the cluster is shown.

shown previously the tertiary carbon site (binding energy 190 cm^{-1}) generates a red shift, the edge site (binding energy 235 cm^{-1}) generates small ($\sim 50\text{ cm}^{-1}$) blue shift, and the nitrogen site (binding energy 200 cm^{-1}) generates a large ($\sim 250\text{ cm}^{-1}$) blue shift.⁵ The spectra and the associated solvation-site shifts are explained in Ref. 5. These data serve to generate expectations for the more complex solvation situations to be discussed below.

2. ABCO/nonpolar solvent clusters

Again for comparison, we present spectra typical of ABCO clustered with nonpolar solvents. Figures 3 and 4 show the MRES of $\text{ABCO}(\text{C}_2\text{H}_4)_1$ and $\text{ABCO}(\text{C}_6\text{H}_{12})_1$, respectively. The features are blue shifted from the ABCO origin (see Table I) and thus represent the case for which the electron in the Rydberg orbital is repelled by the closed shell solvent molecule. In these instances solvent orbitals are not available to accept the excited electron. The spectra presented here are similar to those presented for DABCO.⁵ Note that in some instances the clusters have more than one tran-

TABLE I. Relative spectroscopic shifts of ABCO and DABCO clusters with polar and nonpolar solvents ABCO origin is at $39\,101\text{ cm}^{-1}$. DABCO origin is at $35\,786\text{ cm}^{-1}$ (see Ref. 4).

Solvent	ABCO		DABCO	
	Transition energy (cm^{-1})	Relative shift (cm^{-1})	Transition energy (cm^{-1})	Relative shift (cm^{-1})
Argon	39 332	230	35 891	105
Cyclohexane	39 709	~ 600	36 130	344
Ethylene	38 943	160	35 983	197
Acetonitrile	39 102	~ 0	35 200	-586
1,4-Dioxane	39 102	~ 0	35 600	-186
NH_3	38 585	-516	35 650	-136
$(\text{NH}_3)_2$	38 585	-516		
$(\text{NH}_3)_3$	38 574	-528		
CH_3OCH_3	38 568	-533	35 331	-455
$(\text{CH}_3\text{OCH}_3)_2$	38 561	-541		
THP	38 457	-645	35 511	-275
			35 233	-553
ABCO	38 400	-701	35 101	-685
DABCO			35 245	-541

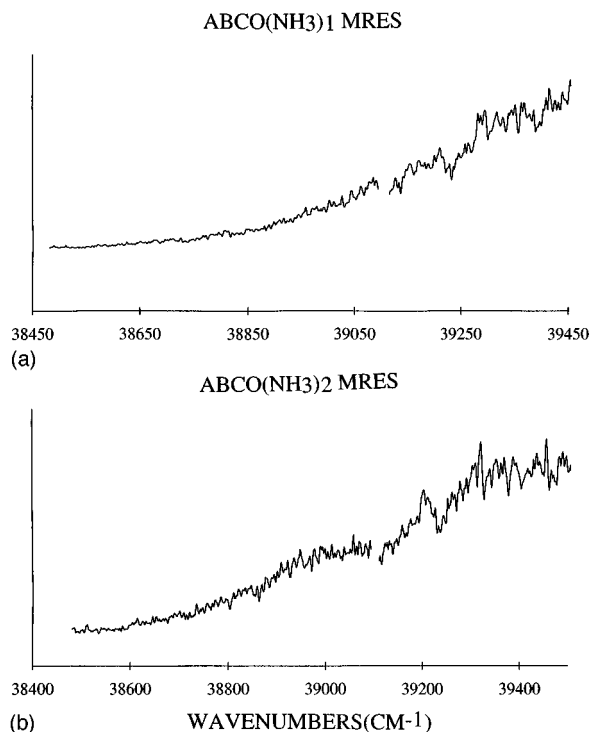


FIG. 5. (a) and (b) The (1+1) MRES of $\text{ABCO}(\text{NH}_3)_{1,2}$ clusters are presented. The red shift of $\text{ABCO}(\text{NH}_3)_1$ $2p3s$ Rydberg state transition is about 516 cm^{-1} . The $\text{ABCO}(\text{NH}_3)_2$ cluster has about the same red shift showing a "saturation" of the electron transfer interaction for only one NH_3 solvent molecule.

sition for what is ostensibly the "origin region;" this is due to multiple cluster structures, most typically the edge and nitrogen solvation sites are occupied. The nitrogen site, of course, has the largest shift (blue or red) because of the solvent proximity to the Rydberg orbital of atomic nitrogen origin.

3. Spectra of ABCO/amine clusters

The spectra of ABCO/amine clusters are typified by $\text{ABCO}(\text{NH}_3)_{1,2}$ and $(\text{ABCO})_2$ cluster spectra. The $\text{ABCO}(\text{NH}_3)_{1,2}$ spectra are presented in Fig. 5(a) and 5(b). They are uniformly broad, featureless and significantly red shifted compared to the ABCO origin and the ABCO/nonpolar molecule and argon clusters. The observed feature has a width (FWHM) of $\sim 1000 \text{ cm}^{-1}$. The transition Franck-Condon factor has changed dramatically from that of the bare molecule and nonpolar clusters. The onset of the transition should be compared to the 0_0^0 feature of the bare molecule to calculate a spectral shift. The size of the red shift is clearly not correlated to the number of solvent molecules present. This observation is opposite to what occurs for nonpolar and rare gas solvent for both ABCO and DABCO.⁵ Table I contains a listing of these shifts.

The $(\text{ABCO})_2$ spectra also present large red shifts for the observed Rydberg transition as expected. The shift is given in Table I. As expected the red shift is largest for the dimer.

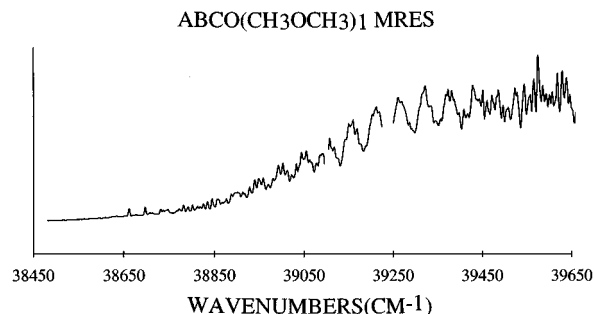


FIG. 6. The (1+1) MRES in the region of the $2p3s$ singlet Rydberg state of the $\text{ABCO}(\text{CH}_3\text{OCH}_3)_1$ is presented. A red shift of about 530 cm^{-1} relative to the ABCO origin is observed.

4. Spectra of ABCO/ether clusters

Figure 6 presents the origin spectrum of the $\text{ABCO}(\text{CH}_3\text{OCH}_3)_1$ cluster. This spectrum is representative of both larger ether clusters, dioxane, and tetrahydropyran (THP) ABCO clusters. Table I lists the observed shifts. The dioxane cluster has no shift and this is probably associated with the details of the electronic and geometric structure of the system. We will discuss this further in the next section. As is the case for ammonia clusters, almost all of the shift is generated by the first solvent molecule.

5. Spectra of ABCO/benzene clusters

The spectrum of DABCO/benzene clusters shows a rich collection of highly red shifted features. Benzene and ABCO, however, absorbed in nearly the same region ($38\,089 \text{ cm}^{-1}$ and $38\,606 \text{ cm}^{-1}$ for 0_0^0 and $0_0^0 + \nu_6$ for benzene and $39\,101 \text{ cm}^{-1}$ for ABCO), so that the spectrum of the solvated ABCO is mixed with that of the solvated benzene. This system is not well suited to the present study and even though interesting results arise from the $\text{ABCO}(\text{C}_6\text{H}_6)_1$ system, the conclusions from these spectra are not straightforward. They will be discussed separately.

C. Excited state dynamics

Lifetimes for the various ABCO clusters and the ABCO monomer are also obtained to determine the evolution of the excited state behavior with time. The lifetime of the first excited Rydberg State of ABCO is $\sim 150 \text{ ns}$ and the decay curve is exponential [Fig. 7(a)]. This measurement is made with the ionization laser set at $\sim 22\,530 \text{ cm}^{-1}$ as the threshold value is $21\,510 \text{ cm}^{-1}$. If the ionization energy is set to $23\,250 \text{ cm}^{-1}$ and the ionization laser is delayed by $\sim 500 \text{ ns}$, the triplet state is accessed and its ionization threshold is $23\,170 \text{ cm}^{-1}$. The triplet state lifetime is too long to measure in this experiment ($> 5 \mu\text{s}$). Figures 8(a) and 8(b) show these thresholds.

The $\text{ABCO}(\text{Ar})_1$ excited singlet state lifetime is 60 ns , probably due to the enhanced intersystem crossing in the cluster. The cluster signal is weak enough so that the triplet

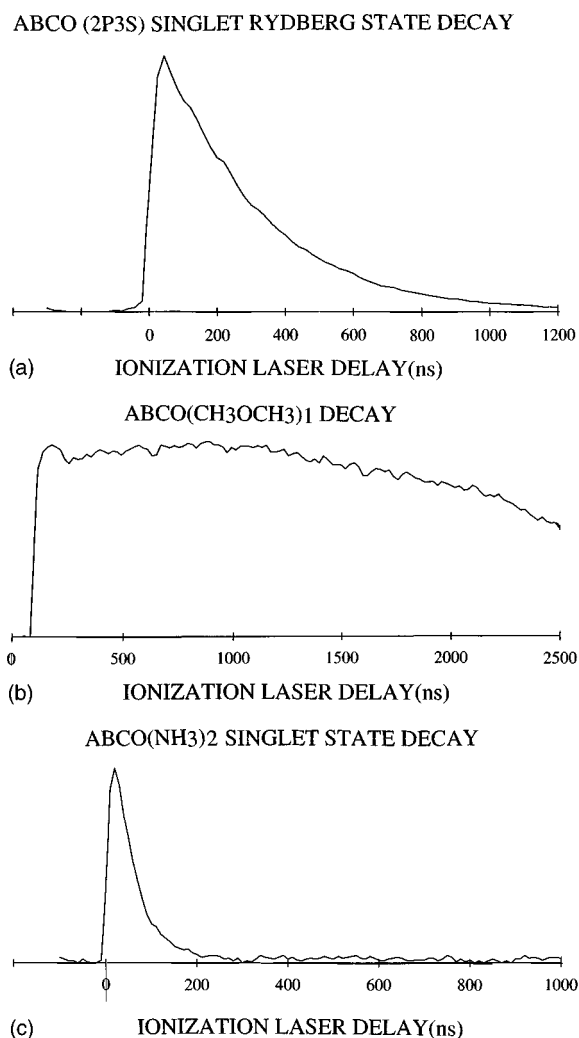


FIG. 7. The $\text{ABCO}(2p3s)$ singlet Rydberg state decay is shown here. The ionization laser is set at about $21\,610\text{ cm}^{-1}$ so that sufficient energy is provided to ionize ABCO. The ionization laser pulse is delayed with respect to the excitation laser to generate this trace. The lifetime of the singlet state is about 200 ns. (b) Lifetime of the $\text{ABCO}(\text{CH}_3\text{OCH}_3)_1$ cluster. The ionization laser energy is set at about 100 cm^{-1} above that required to ionize the cluster origin and is delayed. One can observe that the $\text{ABCO}(\text{CH}_3\text{OCH}_3)_1$ excited state is long lived. This is indicative of an electron transfer state. The tail-off of the signal is due to the detection limit of the instrumentation and does not reflect decay of the electron transfer state. (c) The $\text{ABCO}(\text{NH}_3)_2$ singlet state decay is shown for near threshold ionization for the ABCO bare molecule Rydberg state. This presents the decay of the originally accessed localized singlet state to the long lived electron transfer state. If the ionization energy is increased, the observed decay curve looks like that for $\text{ABCO}(\text{CH}_3\text{OCH}_3)_1$ in (b).

state lifetime could not be measured nor could the dissociated ABCO from the triplet state of the cluster be observed.

Polar solvent/ABCO clusters have a much different excited state time dependence than either the bare molecule or the nonpolar solvent/ABCO cluster. The initially excited state of ABCO/polar solvent clusters decays within 40–50 ns to a long lived state ($\tau > 3\ \mu\text{s}$). This long lived state is observed if the ionization energy is appropriately raised above that of even the triplet state [Fig. 7(b)]. The decay of the $\text{ABCO}(\text{NH}_3)_2$ cluster obtained with near threshold ionization

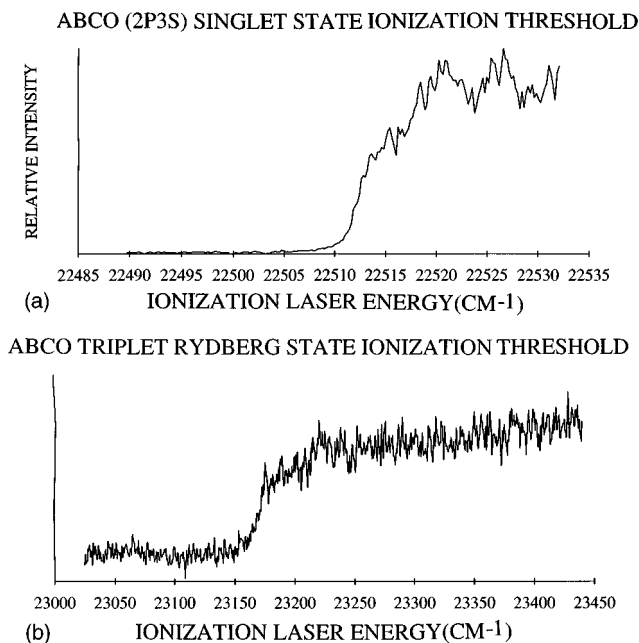


FIG. 8. The ionization threshold of the ABCO bare molecule. The threshold is sharp, $\sim 5\text{ cm}^{-1}$, and is indicative of a Rydberg state ionization threshold. The threshold value is $21\,510\text{ cm}^{-1}$. (b) The ionization threshold of the triplet state of ABCO is $23\,170\text{ cm}^{-1}$. The threshold spectrum is obtained after a 500 ns delay between excitation and ionization lasers.

laser energy for the ABCO monomer shows the rapid loss of the initially excited state [Fig. 7(c)]. The long lived charge transfer state is observed if the ionization energy is raised above the threshold value for this state.

IV. DISCUSSION

A. General observations

We have previously demonstrated,⁹ in considerable depth and detail, that DABCO/polar solvent clusters form low lying electron transfer states that can be identified through both static spectra and dynamics. With these present studies we show that the occurrence of electron transfer reactions for cyclic amines is a more general phenomenon.

Based on the amines ABCO, DABCO, and HMT a number of interactions can be characterized for Rydberg states in clusters. First, and perhaps most generally, a Pauli exclusion or exchange repulsion can be characterized. This interaction can be so large as to destabilize the cluster in the excited state. Second, a van der Waals dispersion interaction occurs and is responsible, in part, for the ground and excited state binding energy of the nonpolar solvent cluster. Third, an attractive dipole–dipole or dipole-induced dipole interaction further stabilizes the cluster in both ground and excited states. These three interactions are by-in-large additive. One observes these effects for nonpolar solvent clusters. The fourth interaction which is responsible for the lowering of the charge or electron transfer state, is the exchange interaction for cluster systems with spatially and energetically available empty solvent orbitals. These solvent orbitals are near the $3s$ Rydberg orbital in both space and energy and can mix

with it to delocalize the excited electron. As these orbitals reduce in overlap and become more distant in energy, the weakened delocalization can be thought of an excitation exchange.

In the cases of these cyclic amines, the mixing must be small and the barrier to the delocalization must be large because the states are seen to evolve in time and the evolution times are on the 40–300 ns time scale.

To generalize these results further, we have also studied this solute/solvent electron transfer reaction for a cyclic ether, 1,4-dioxane.¹⁴ In this case NH_3 , CH_3OH , $\text{C}_3\text{H}_7\text{OH}$, CH_3OCH_3 are employed as the polar solvents for dioxane. The spectra are very broad, very red shifted and very weak as might be anticipated for a strong electron transfer interaction. Time dependent behavior would not be expected on the nanosecond time scale for these clusters because that electron transfer state seems to be accessed directly with a small Franck–Condon factor. Any time dependence for these systems would be expected on the picosecond or subpicosecond timescale and would be interesting to explore.

B. Comparison between ABCO and DABCO clusters

The results in detail for the ABCO and DABCO clusters are not identical as can be seen from Table I and a cursory look at the respective lifetimes. The electron transfer develops in ~ 40 ns for ABCO but as much as 250 ns for DABCO. Perhaps, the most obvious general comparison between the two systems is that the shifts (either red or blue) are larger for ABCO than DABCO and that the electron transfer times and lifetimes for DABCO are much larger than for ABCO. One is initially tempted to attribute these differences to the presence of an ABCO (C_{3v} symmetry) dipole moment and transition dipole moment; however, the dipole–dipole interaction is attractive and should thus reduce, not increase, the blue shift due to exchange repulsion for ABCO over DABCO clusters. This latter result is seen for DABCO/propane, thioether, and ether clusters.⁹ In any event this expected trend is not obvious and shifts do not necessarily correlate with dipolar behavior. Lifetimes, too, do not follow a specific dipolar expectation, although the general trend does seem to hold that ABCO electron transfer times are about a factor of 4 faster than DABCO electron transfer times.

Clearly these effects and differences are more subtle than semiclassical multipolar interactions provide for and must be treated at a detailed *ab initio* level in order to generate productive understanding of these observations. We plan to pursue *ab initio* calculations to determine the potential surface appropriate for such phenomena in the near future. The behavior we observe for these systems depends on the detailed geometry and orbital overlap for each individual cluster.

An additional difference between ABCO and DABCO cluster behavior can be found in their geometry. ABCO/polar solvent clusters seem to prefer an edge solvation geometry while DABCO/polar solvent clusters prefer solvation at the nitrogen end site. Moreover, DABCO/ $C_n\text{H}_{2n+2}$ clusters switch from edge to nitrogen end coordination at approxi-

mately $n=2$.⁵ Perhaps these subtleties will also arise from careful and extensive *ab initio* calculations. At present the underlying reasons for these structural differences and changes are not clear.

V. CONCLUSIONS

The electron transfer state and electron transfer dynamics reported for DABCO/polar solvent clusters are explored and generalized for ABCO/polar solvent clusters. These same properties and phenomena are also characterized for dioxane (a cyclic ether) clustered with the same solvents. Thus, the overall electron transfer behavior for Rydberg states of molecules solvated with ethers, alcohols, aromatics, and amines is shown to be quite general. As demonstrated, one-to-one clusters are an excellent vehicle for the study of this type of elementary chemical reaction.

The experimental observations for these clusters include spectral shifts from the isolated chromophore molecule features, linewidths, lifetimes, ionization energy, and ionization threshold shapes. These data have facilitated the identification of a number of limiting forms of solute–solvent interaction; van der Waals dispersion interactions, dipolar interactions, exchange repulsion (Pauli Exclusion Principle) interaction, and exchange delocalization or electron transfer interactions. The first three of these interaction forms are qualitatively additive for the $2p3s$ Rydberg states of amines and ethers. The electron delocalization or transfer process takes place for solvent molecules that have available orbitals that spatially and energetically overlap well with the chromophore $2p3s$ Rydberg state. The dynamics of the electron transfer process suggest that a large barrier exists for DABCO/solvent clusters and that the barrier is somewhat smaller for ABCO/solvent clusters. The dioxane/solvent clusters seem to have a much reduced barrier as the electron transfer states appear to be directly accessed by $S_1 \leftarrow S_0$ excitation.

We have located the ABCO triplet state through delayed ionization studies and found the triplet Rydberg state ~ 650 cm^{-1} below the singlet. This is within ~ 100 cm^{-1} of the relative location of the DABCO Rydberg triplet state. The small singlet/triplet splitting for the Rydberg state is to be expected because the Rydberg electron interacts only weakly with the core electrons.

Empirical potential energy calculations of cluster structure and binding energies are of enormous help in analyzing the experimental data and focusing our thinking about the intermolecular interactions in these clusters. Such calculations demonstrate that three binding sites are relevant for ABCO clusters, between the C–C bridge, at the nitrogen atom, and at the tertiary carbon end of ABCO. Shifts and interactions correlate with these structures. The calculations show the ABCO and DABCO cluster structures are similar but the largest interaction between these molecules and solvents occurs for different solvation sites. DABCO/polar solvent clusters have the lowest energy geometry for the nitrogen atom site while the side or edge solvation site is most tightly bound for the ABCO system.

A detailed mechanistic understanding of these structures and dynamics will only arise through extensive *ab initio* calculations, which we are presently pursuing.

With this effort we have demonstrated the generality and importance of the electron transfer process for excited Rydberg states in a solvation environment.

ACKNOWLEDGMENT

These studies are supported by the USARO.

¹See, for example, *Atomic and Molecular Clusters*, edited by E. R. Bernstein (Elsevier, Amsterdam, 1990).

²R. Disselkamp, and E. R. Bernstein, *J. Chem. Phys.* **98**, 4339 (1993).

³J. A. Menapace and E. R. Bernstein, *J. Phys. Chem.* **91**, 2533 (1987).

⁴Q. Y. Shang, P. O. Moreno, S. Li, and E. R. Bernstein, *J. Chem. Phys.* **98**, 1876 (1993).

⁵Q. Y. Shang, P. O. Moreno, C. F. Dion, and E. R. Bernstein, *J. Chem. Phys.* **98**, 6769 (1993).

⁶Q. Y. Shang, C. F. Dion, and E. R. Bernstein, *J. Chem. Phys.* **101**, 118 (1994).

⁷P. O. Moreno, Q. Y. Shang, and E. R. Bernstein, *J. Chem. Phys.* **97**, 2869 (1992).

⁸R. Disselkamp, Q. Y. Shang, and E. R. Bernstein, *J. Phys. Chem.* **99**, 7227 (1995).

⁹Q. Y. Shang, P. O. Moreno, and E. R. Bernstein, *J. Am. Chem. Soc.* **116**, 302 (1994).

¹⁰(a) K. Law, M. Schauer, and E. R. Bernstein, *J. Chem. Phys.* **80**, 207 (1984); (b) For a good general reference, see D. H. Levy, *Adv. Chem. Phys.* **47** (pt 1), 323 (1981).

¹¹S. Li and E. R. Bernstein, *J. Chem. Phys.* **95**, 1577 (1991).

¹²G. Nemethy, M. S. Pottle, and H. A. Scheraga, *J. Phys. Chem.* **87**, 1883 (1983).

¹³J. J. P. Stewart, *A General Molecular Orbital Package*, 6th ed. QCPE, No. 455 (1989).

¹⁴C. F. Dion and E. R. Bernstein (unpublished results).